Indian Journal of Chemistry
Vol. 65, January 2026, pp. 11-17
DOI: 10.56042/ijc.v65i1.18547

Synthesis, characterization and antimicrobial studies of novel Schiff base and its 3d series metal complexes

K Ramya Charitha & P Kavitha*

Department of Chemistry, Chaitanya (Deemed to be University), Hyderabad 506 001, Telangana, India

E-mail: kavithapingili04@gmail.com

Received 4 April 2025; accepted (revised) 27 November 2025

This paper describes the synthesis, characterisation, and antimicrobial evaluation of a Schiff base ligand 3-hydroxy-4-[(1E)-[(6-sulfanylpyrimidin-4-yl)imino]methyl]benzonitrile (LH), as well as its Mn(II), Fe(II), Co(II), Ni(II), Cu(II) and Zn(II) metal complexes. The ligand has been created by combining 6-aminopyrimidine-4-thiol and 4-formyl-3-hydroxybenzonitrile in ethanol under reflux conditions, using acetic acid as a catalyst. The production of the ligand and its complexes have been validated using spectroscopy and other analytical methods. The antibacterial activity of these compounds have been tested against Gram-positive and Gram-negative bacterial strains utilizing agar diffusion techniques. Additionally, antifungal activity has been tested against *T. reesei* and *C. albicans* using the agar well diffusion technique. The generated metal complexes exhibit higher antibacterial activity than the free ligand, implying potential use in antimicrobial drug development.

Keywords: Schiff base, 3d series metals, Coordination chemistry, Antibacterial activity, Antifungal studies

In contemporary research, azomethine ligands and three-dimensional metal complexes are essential, impacting both theoretical and applied chemistry[1]. The imine group's flexibility and simplicity of synthesis make it essential in coordination chemistry[2,3]. Usually produced through carbonyl-amino interactions, Schiff bases are crucial ligands in metal coordination[4-6]. Their metal complexes have demonstrated enzymatic, antibacterial and anticancer characteristics, which makes them useful for therapeutic uses[7,8]. Many studies have been conducted on these complexes for their ability to bind oxygen, reduce alkenes, exhibit photochemical activity and chelate metals[9–11]. Many Schiff bases are of increasing interest in material science and drug research[12–16] due to their antiseptic, anticancer and antibiotic qualities[17–19].

Schiff base-metal complexes are used in green chemistry, wastewater treatment and catalysis[20–24]. They work well as catalysts in organic reactions because of their stability and coordination abilities. Additionally, they enhance the thermal and electrical characteristics of optoelectronics, sensors, and energy storage through their application in nanomaterials, composite materials, and functional coatings[25–29]. Furthermore, a great deal of research has been done on their bioinorganic potential in medicinal chemistry and diagnostics[30–34]. These complexes help create supramolecular structures with special magnetic and photophysical characteristics that are helpful in nanotechnology and molecular circuits[35–37]. Schiff base-metal compounds are still being investigated by researchers for potential industrial and biological applications.

By raising lipid affinity, rupturing microbial membranes, blocking enzymes and producing reactive oxygen species (ROS), which cause cell death, Schiff base metal complexes show more pronounced antimicrobial actions[38–43]. Metals such as Cu, Ni, Co, Zn, and Fe affect toxicity, redox potential, and coordination behaviour, and their activity extends to a variety of bacterial and fungal strains[44–47]. Zn complexes exhibit potent antibacterial and antifungal qualities, but Cu(II) complexes intensify oxidative stress. Stability and bioactivity are influenced by structural elements including substituents, oxidation state and ligand electronics[48–51]. They are prospective substitutes for antibiotics due to their selective toxicity, biofilm inhibition, and effectiveness against drug-resistant bacteria, according to studies[52–54]. In order to improve current antibiotics and prevent the emergence of resistance, Schiff base metal complexes are being investigated for combination therapy[55–57].

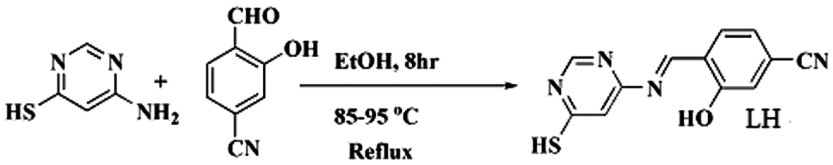

Scheme 1

In this work, a Schiff base ligand LH and its Mn(II), Fe(II), Co(II), Ni(II), Cu(II) and Zn(II) complexes are synthesized, characterized and evaluated for antimicrobial activity. Tests of their antibacterial and antifungal properties showed that the metal complexes were more effective.

Materials and Methods

We purchased all necessary chemicals from Sigma-Aldrich and used them exactly as supplied, requiring no additional purification. Solvents and metal salts were purchased from E. Merck and used in their original form. The course of the reaction was tracked using TLC on silica-gel plates (Merck, India). Using a Perkin Elmer 1650 spectrophotometer, IR spectra were captured using KBr pellets in the 4000–400 cm^{-1} range. TMS was used as the internal reference and DMSO-d_6 as the solvent to generate nuclear magnetic resonance (^{1}H and ^{13}C NMR) spectra on a Varian 400 MHz spectrometer. A 70 eV Agilent 5973 mass spectrometer was used for the mass spectrometric analysis. Samples were heated at a rate of 2°C/min from 30 to 1000°C for TGA using a Universal TGA Q50. UV-Vis: Shimadzu UV-2600, PerkinElmer Lambda 365 (200-1200 nm). VSM: Lake Shore 7400 Series (Magnetic Moment Measurement).

Synthesis

Synthesis of ligand (LH)

1.34 grams (0.1M) 6-aminopyrimidine-4-thiol and 1.56 grams (0.1M) 4-formyl-3-hydroxybenzonitrile were dissolved in 15 mL of ethanol to create the chemical 3-hydroxy-4-[(1E)-[(6-sulfanylpyrimidin-4-yl)imino]methyl]benzonitrile (LH). The procedure was carried out in a round bottom flask. The liquid turned yellow after eight hours of constant stirring and heating with a tiny bit of acetic acid. TLC was used to monitor the progress of the reaction. The reaction was carried out by lowering the solution's pressure during evaporation, washing the yellow precipitate with ethanol, filtering and then using ethanol to recrystallize the resulting product[58-61] (Scheme 1).

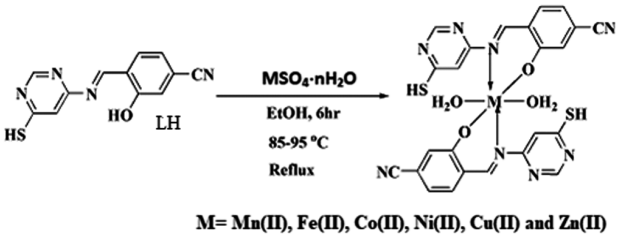

Scheme 2

Anlytical data: Mol. Formula $C_{12}H_8N_4OS$. Colour: yellow solid. Yield 84%. m.p.247.32-249.45°C. ^{1}H NMR (400 MHz, DMSO-d_6): δ 3.86 (s, 1H, SH), 7.01 (d, 1H, Ar, J = 8MHz), 7.40 (s, 1H, Ar), 7.70 (m, 2H, Ar), 8.36 (s, 1H, Ar), 8.69 (s, 1H, imine-CH), 10.17 (s, 1H, OH); ^{13}C NMR (400 MHz, DMSO-d_6): δ 196.02 (SH-C), 190.22 (C-N-Ar), 165.62 (imine C), 160.78, 150.15 (pyramidine-C), 134.15, 133.12, 127.60, 117.68, 115.38 (CN), 103.32, 95.38; IR (KBr): 1704 (C=N), 1180 (C-O), 3515 (OH), 1563 (C=C), 765 (C-S) cm^{-1}; MS: *m/z* 256.64 $[M]^+$. Anal. Ligand (LH): Calcd: C, 56.21; H, 3.17; N, 21.83. Found: C, 56.24; H, 3.15; N, 21.86%. UV-Vis: 282, 383 nm.

Synthesis of 3d series metal complexes

Metal Chelates were synthesized by mixing the ligand (0.01M) LH with the Mn(II), Fe(II), Co(II), Ni(II), Cu(II) and Zn(II) metal salts in a 1:2 (M:L) ratio. The metal salts (0.01 M) were dissolved separately in distilled water and pure HCl, and the prepared metal solution is added drop by drop to the 10 mL of ethanolic ligand solution. To maintain a constant *p*H 4-5 drops of sodium acetate solution were added, after agitation and refluxing the mixture on a magnetic stirrer with a hot plate for four hours, formation of a solid deposit resulted. Ethanol was used to rinse it after filtering out the solid and let it dry. Every metal ligand product was examined for characterisation[62-65] (Scheme 2).

Mn complex: ^{1}H NMR (400 MHz, DMSO-d_6): δ 3.96 (s, 2H, 2×SH), 4.67 (s, 4H, 2×H_2O), 7.15 (d, 2H, Ar, J = 8MHz), 7.56 (s, 2H, Ar), 7.84 (m, 4H, Ar), 8.47 (s, 2H, Ar), 8.86 (s, 2H, imine-CH); ^{13}C NMR (400 MHz, DMSO-d_6): δ 197.56 (SH-C), 196.35, 190.26,

189.78 (C-N-Ar) (Ar - C), 165.45 (imine C), 160.32, 149.89 (pyramidine-C), 130.39, 130.41, 128.15, 118.06, 115.08 (CN), 112.27, 110.08, 103.29, 102.59, 95.49; IR (KBr): 1658 (C=N), 1147 (C-O), 3380 (H_2O), 1533 (C=C), 754 (C-S), 661 (M-O), 528 (M-N); MS: *m/z* 601.2 $[M]^+$. Anal. Calcd: C, 47.92; H, 3.02; N, 18.63. Found: C, 47.89; H, 3.05; N, 18.60%. UV-Vis: 504, 1121 nm. Magnetic moment BM: 5.92. Paramagnetic.

Fe(II) complex: Mol. Formula $FeC_{24}H_{18}N_8O_4S_2$, Colour: Purple, Yield 67%. m.p.229.51-231.63°C. ^{1}H NMR (400 MHz, DMSO-d_6): δ 3.92 (s, 2H, 2×SH), 4.63 (s, 4H, 2×H_2O), 7.13 (d, 2H, Ar, *J* = 8MHz), 7.52 (s, 2H, Ar), 7.80 (m, 4H, Ar), 8.43 (s, 2H, Ar), 8.82 (s, 2H, imine-CH). ^{13}C NMR (400 MHz, DMSO-d_6): δ 197.09 (SH-C), 196.12 (SH-C), 190.21, 189.96 (C-N-Ar) (Ar - C), 165.11 (imine C), 160.18, 150.08 (pyramidine-C), 130.36, 130.38, 128.12, 118.03, 115.06 (CN), 112.21, 110.02, 103.31, 102.56, 95.03; IR (KBr): 1661(C=N), 1114(C-O), 3321(H_2O), 1512 (C=C), 759(C-S), 657(M-O), 521(M-N); MS: *m/z* 602.09 $[M]^+$. Anal. Calcd: C, 47.83; H, 2.98; N, 18.63. Found: C, 47.85; H, 3.01; N, 18.60%. UV-Vis: 447, 672 nm. Magnetic moment BM: 4.90. Paramagnetic.

Co(II) complex: Mol. Formula $CoC_{24}H_{18}N_8O_4S_2$. Colour: Red. Yield 69%. m.p.235.43-237.59°C. ^{1}H NMR (400 MHz, DMSO-d_6): δ 3.88 (s, 2H, 2×SH), 4.63 (s, 4H, 2×H_2O), 7.22 (d, 2H, Ar, *J* = 8MHz), 7.57 (s, 2H, Ar), 7.87 (m, 4H, Ar), 8.49 (s, 2H, Ar), 8.94 (s, 2H, imine-CH). ^{13}C NMR (400 MHz, DMSO-d_6, δ ppm): 196.10, 195.13 (SH-C), 189.98, 189.19 (C-N-Ar), 165.06 (imine C), 160.23, 149.96 (pyramidine-Cs), 134.98, 133.86, 127.82, 116.60, 114.96 (CN), 111.89, 109.67, 102.23, 101.31, 94.99; IR (KBr): 1686 (C=N), 1167 (C-O), 3383 (H_2O), 1524 (C=C), 759 (C-S), 650 (M-O), 530 (M-N); MS: *m/z* 605.22 $[M]^+$. Anal. Calcd: C, 47.58; H, 3.02; N, 18.47. Found: C, 47.61; H, 3.00; N, 18.51%. UV-Vis: 257, 347 nm. Magnetic moment BM: 3.87. Paramagnetic.

Ni(II) complex: Mol. Formula $NiC_{24}H_{18}N_8O_4S_2$. Colour: Violet. Yield 64%. m.p.223.23-225.43°C. ^{1}H NMR (400 MHz, DMSO-d_6): δ 3.84 (s, 2H, 2×SH), 4.64 (s, 4H, 2×H_2O), 7.10 (d, 2H, Ar, *J* = 8MHz), 7.48 (s, 2H, Ar), 7.77 (m, 4H, Ar), 8.37 (s, 2H, Ar), 8.87 (s, 2H, imine-CH). ^{13}C NMR (400 MHz, DMSO-d_6): δ 195.09, 194.12 (SH-C), 186.48, 185.86 (C-N-Ar), 165.06 (imine-C), 160.11, 148.51 (pyramidine-Cs), 134.62, 133.53, 128.23, 116.03, 114.62 (CN), 111.04, 109.37, 102.23, 101.36, 95.06; IR (KBr): 1662 (C=N), 1165 (C-O), 3450 (H_2O), 1518 (C=C), 771 (C-S), 600 (M-O), 542 (M-N); MS: *m/z* 605.60 $[M]^+$. Anal. Calcd: C, 47.60; H, 2.97; N, 18.53. Found: C, 47.62; H, 3.00; N, 18.51%. UV-Vis: 295, 407 nm. Magnetic moment BM: 2.83. Paramagnetic.

Cu complex: ^{1}H NMR (400 MHz, DMSO-d_6): δ3.78 (s, 2H, SH), 4.58 (s, 4H, H_2O), 7.04 (d, 2H, Ar, J = 8 MHz), 7.42 (s, 2H, Ar), 7.71 (m, 4H, Ar), 8.31 (s, 2H, Ar), 8.81 (-CH=N) proton is detected at 8.81 ppm. ^{13}C NMR (400 MHz, DMSO-d_6): δ 196.93 (SH-C), 195.35, 190.06, 189.56 (C-N-Ar) (Ar - C), 165.04 (imine C), 160.42, 150.12 (Pyramidine-C), 134.56, 133.47, 128.17, 118.34, 115.97 (CN), 114.56, 110.98, 103.31, 102.71, 95.02; IR (KBr): 1670 (C=N), 1172 (C-O), 3357 (H_2O), 1508 (C=C), 755 (C-S), 645 (M-O), 581 (M-N); MS: *m/z* 609.1 $[M]^+$. Anal. Calcd: C, 47.25; H, 2.97; N, 8.37. Found: C, 47.21; H, 2.94; N, 8.39%. UV-Vis: 262, 383 nm. Magnetic moment BM: 1.73. Paramagnetic.

Zn complex: ^{1}H NMR (400 MHz, DMSO-d_6): δ 3.75 (s, 2H, SH), 4.55 (s, 4H, H_2O). 7.01 (d, 2H, Ar, J = 8 MHz), 7.39 (s, 2H, Ar), 7.68 (m, 4H, Ar), 8.28 (s, 2H, Ar), 8.78 ppm (-CH=N). ^{13}C NMR (400 MHz, DMSO-d_6): δ 195.00 (SH-C), 194.03, 186.39, 185.77 (C-N-Ar), 164.97 (-C=N), 160.02 and 148.42 (Pyramidine-C), 134.53, 133.44, 128.14, 115.94 (CN, 114.53, 110.95, 103.13, 102.57, 94.97; IR (KBr): 1675 (C=N), 1171 (C-O), 3359 (H_2O), 1536 (C=C), 741 (C-S), 653 (M-O), 557 (M-N); MS: *m/z* 610.3 $[M]^+$. Anal. Calcd: C, 47.10; H, 2.96; N, 18.31. Found: C, 47.07; H, 2.94; N, 18.27%. UV-Vis: 454, 667 nm. Magnetic moment BM: 0. Diamagnetic.

Antimicrobial studies

Antibacterial studies

The bacteria chosen for this study are Gram positive (*B. cereus*, *M. luteus*, *S. aureus*) and Gram negative (*K. pneumoniae*, *E. aerogenes*, *E. coli*, *P. fluorescens*, *P. aeruginosa*, *S.enteritidis*). The bacterial stock cultures which were kept at 4°C in a freezer were used for testing. The antibacterial capabilities of the LH and its coordination compounds were systematically examined through agar-based diffusion assays. Nine foodborne bacterial pathogens were inoculated onto nutrient agar under carefully monitored settings. After that, samples (1 mg/mL) dissolved in DMSO were placed in sterilized discs with wells 6 mm in

diameter[66–68]. After drying, the discs were placed on inoculation plates and incubated for 24 to 48 hours at 37°C. The zone of inhibition was used to determine the lowest concentration that would still prevent the microorganism's activity from growing.

Antifungal assays

In order to study the antifungal properties of the synthesized compounds, the agar well diffusion technique was employed against *T. reesei* and *C. albicans*. After inoculating the PDA agar medium with a fungal culture using a sterile swab, 6 mm wells were made and filled with a solution of the test compound at concentrations between 20 g/mL and 80 g/mL. The plates were allowed to air dry for 15 minutes and then incubated at 30°C. The effectiveness of the compounds was assessed by measuring the size of the inhibitory zones after 2 days of incubation. Ketoconazole was used as the standard reference for comparison[69,70].

Results and Discussion

Chemistry

In the present investigation, 4-formyl-3-hydroxybenzonitrile and 6-aminopyrimidine-4-thiol were heated and agitated in ethanol to form the ligand 3-hydroxy-4-[(1E)-[(6-sulfanylpyrimidin-4-yl)imino] methyl]benzonitrile (LH), which was subsequently purified by recrystallization. Metal complexes of Mn(II), Fe(II), Co(II), Ni(II), Cu(II) and Zn(II) were created by reacting metal chlorides with the ligand in a 1:2 ratio when reflux was present. The resulting precipitates were filtered, washed, and dried for further spectrum characterization. According to the ^{1}H NMR spectrum data, the Schiff base ligand (LH) is coordinated with the metal centres Mn(II), Fe(II), Co(II), Ni(II), Cu(II) and Zn(II). When the imine proton (-CH=N) shifts from 8.69 ppm (ligand) to 8.86 ppm (Mn), 8.82 ppm (Fe), 8.94 ppm (Co), 8.87 ppm (Ni), 8.81(Cu) ppm and 8.78 ppm (Zn) it indicates metal binding and a deshielding effect caused by the removal of electron density. Aromatic protons shift to 7.13–8.43 ppm (Fe), 7.22–8.49 ppm (Co), and 7.10–8.37 ppm (Ni), 7.15-8.47 ppm (Mn), 7.08-8.31 ppm (Cu) and 7.01-8.28 ppm (Zn) from 7.01–8.36 ppm. These modifications illustrate how the steric environment has evolved due to metal-ligand π interactions. These changes are consistent with successful complex formation and changes in the strength of the metal-ligand link.

Mass spectra

According to the mass spectroscopy technique, the imine base and Mn(II), Fe(II), Co(II), Ni(II), Cu(II) and Zn(II) complexes were successfully produced. Its presence and structural integrity were confirmed by the discovery of the ligand at *m/z* = 256.64, which is equivalent to its estimated molecular mass. The interaction of the metal ions with the ligand was also confirmed by peaks at *m/z* = 601.2, 602.09, 605.22, 605.60, 609.1 and 610.3 which show Mn, Fe, Co, Ni, Cu and Zn complexation. Their structural characterization is further supported by these results, which provide strong evidence of metal-ligand coordination and stable metal complex formation.

IR spectra

The IR spectral analysis confirms successful coordination of the ligand with Mn(II), Fe(II), Co(II), Ni(II), Cu(II) and Zn(II) metal ions. The ligand shows characteristic absorption bands at 1704 cm^{-1} (C=N), 1180 cm^{-1} (C-O), 3515 cm^{-1} (O-H), 1563 cm^{-1} (C=C), and 765 cm^{-1} (C-S). Upon complexation, notable shifts are observed, confirming the involvement of azomethine nitrogen and phenolic oxygen in metal coordination. The C=N stretching vibrations shift to lower frequencies (1661–1686 cm^{-1}), while the C-O bands shift to lower wavenumbers (1114–1172 cm^{-1}), indicating interaction with metal centres. The O-H stretching frequency decreases significantly (3321–3450 cm^{-1}), suggesting the presence of coordinated water molecules. The C=C and C-S bands also show minor shifts, reflecting electronic changes upon complexation. The appearance of new bands in the 600–661 cm^{-1} (M-O) and 521–581 cm^{-1} (M-N) regions confirms metal-ligand bond formation. The overall spectral shifts provide strong evidence of successful complexation, with each metal ion influencing the ligand's electronic environment differently (Table 1).

Thermal analysis

TGA is an essential method used to investigate metal complex's resistance to heat and patterns of breakdown. The TGA curves for the metal complexes of Mn(II), Fe(II), Co(II), Ni(II), Cu(II) and Zn(II) show temperature-driven mass loss and provide insights into the metal's possible ligand-metal interactions, thermal degradation and structural integrity[57,58].

Table 1 — IR spectral data of ligand LH and Mn, Fe, Co, Ni, Cu, and Zn complexes (cm^{-1})

S. No.	Compd	C=N	C-O	O-H/H_2O	C=C	C-S	M-O	M-N
1	Ligand	1704	1180	3515	1563	765	–	–
2	Mn(II)	1658	1147	3380	1533	754	661	528
2	Fe(II)	1661	1114	3321	1512	759	657	521
3	Co(II)	1686	1167	3383	1524	759	650	530
4	Ni(II)	1662	1165	3450	1518	771	600	542
6	Cu(II)	1670	1172	3357	1508	755	645	581
7	Zn(II)	1675	1171	3359	1536	741	653	557

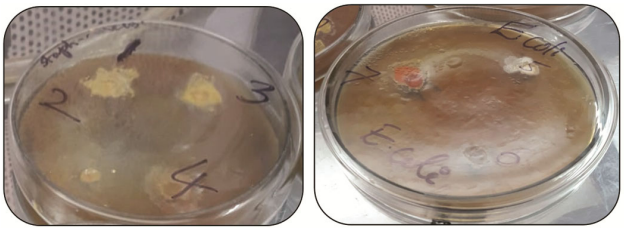

Fig. 1 — Selected photographs of *in vitro* anti-bacterial activity of compounds

The thermal analysis of the metal complexes reveals a multi-stage decomposition pattern, indicating their stability. Initial mass loss below 150°C corresponds to weakly bound water removal. Coordinated solvent molecules decompose between 150–250°C, requiring more energy due to strong metal-ligand interactions. Major ligand degradation occurs beyond 600°C, leading to the final residue formation at 800–980°C. The Ni(II) complex exhibits the highest thermal stability (940°C), followed by Co(II) and Cu(II) (900°C), while Mn(II) and Fe(II) degrade around 800°C. The Zn(II) complex decomposes above 980°C but shows gradual weight loss, indicating lower structural rigidity. Overall, the stability order follows Ni(II) > Co(II) ≈ Cu(II) > Mn(II) ≈ Fe(II) > Zn(II). These results suggest potential applications in catalysis and material science, particularly for thermally stable complexes.

Antimicrobial investigations

Antibacterial assays

A larger zone of inhibition signifies enhanced antibacterial strength. Ciprofloxacin, a widely used fluoroquinolone antibiotic, served as the standard in this study. The synthesized ligand (LH) and its Metal (II) complexes exhibited distinct levels of antimicrobial action against different bacterial species.

The ligand (LH) demonstrated notable antibacterial activity, particularly against *S. aureus* (MIC: 3.15 mg/mL), *E. coli* (1.18 mg/mL), and *S. enteritidis* (2.28 mg/mL). Metal complexes of Co(II), Ni(II), and Cu(II) exhibited enhanced antibacterial effects. Specifically, the Co(II) complex showed activity against *S. aureus* (MIC: 2.54 mg/mL) and *E. aerogenes* (2.20 mg/mL); the Ni(II) complex against *S. aureus* (3.10 mg/mL); and the Cu(II) complex against *S. aureus* (3.12 mg/mL), *E. aerogenes* (2.11 mg/mL), *E. coli* (1.15 mg/mL), *P. fluorescens* (2.25 mg/mL), and *S. enteritidis* (1.64 mg/mL). The Fe(II) and Zn(II) complexes displayed good activity, with the Fe(II) complex effective against *K. pneumoniae* (MIC: 4.12 mg/mL) and *E. coli* (1.14 mg/mL), and the Zn(II) complex against *K. pneumoniae* (3.16 mg/mL). Mn(II) showed moderate activity in when compared, but decent activity was reported against *E. coli* (MIC: 1.10 mg/mL) (Fig. 1, Table 2). The increased efficacy of these complexes is attributed to strong metal-ligand interactions facilitating bacterial cell membrane penetration, metabolic disruption, and reactive oxygen species generation. The presence of heterocyclic moieties and improved solubility further contribute to their antibacterial potency. These findings suggest that metal coordination enhances the antibacterial properties of the ligand, with Co(II), Ni(II), and Cu(II) complexes showing the most significant improvements.

Cu(II) and Fe(II) complexes exhibit enhanced antibacterial activity compared to their parent ligands, likely due to strong metal-ligand interactions and increased bacterial membrane permeability. This suggests their potential as effective antimicrobial agents.

Antifungal potential

The antifungal activity of the ligand (LH) and its metal complexes against *T. reesei* and *C. albicans* was evaluated at two different concentrations (80µg/mL and 60µg/mL). The results were compared with *Amphotericin B* as the standard antifungal agent.

Table 2 — MIC of ligand and its metal complexes (mg/mL) (NA= not active)

Antibacterial Activity		MIC (mg/mL) Ciprofloxacin	LH	Mn(II)	Fe(II)	Co(II)	Ni(II)	Cu(II)	Zn(II)
Gram positive	*Bacillus cereus*	1.41	2.65	NA	NA	2.21	2.09	2.21	NA
	Micrococcus luteus	2.22	NA	4.11	3.11	4.54	4.21	3.54	3.63
	Staphylococcus aureus	3.17	3.15	NA	NA	2.54	3.10	3.12	NA
Gram negative	*Klebsiella pneumoniae*	4.14	4.16	4.45	4.12	4.83	4.76	4.73	3.61
	Enterobacter aerogenes	2.12	2.46	NA	NA	2.20	NA	2.11	NA
	Escherichia coli	1.18	1.18	1.10	1.14	3.97	3.98	1.15	2.91
	Pseudomonas fluorescens	3.07	NA	NA	NA	5.36	4.86	5.76	4.66
	Pseudomonas aeruginosa	2.45	2.56	NA	NA	2.28	NA	2.25	NA
	Salmonella enteritidis	2.11	2.28	2.34	2.34	3.36	1.84	1.64	3.34

Table 3 — Antifungal activities of LH ligand and its metal complexes

Compd	Zone of inhibition (mm)		
	Conc. (μg/mL)	*T. reesei*	*C. albicans*
Ligand (LH)	80	29	25
	60	26	21
Mn complex	80	22	24
	60	18	21
Fe Complex	80	32	31
	60	28	29
Co complex	80	30	26
	60	28	22
Ni complex	80	29	20
	60	26	17
Cu complex	80	34	30
	60	28	28
Zn complex	80	32	31
	60	30	29
Amphotericin B	80	27	26
	60	25	23

The Cu(II) complex exhibited the highest inhibition zones, measuring 34 mm against *T. reesei* and 30 mm against *C. albicans* at 80 μg/mL, likely due to its enhanced coordination properties facilitating greater cellular disruption in test organisms. Similarly, the Zn(II) complex showed significant effects with inhibition zones of 32 mm and 31 mm, respectively, attributed to its strong binding affinity with biomolecules. The Fe(II) complex also displayed considerable activity, with inhibition zones of 32 mm and 31 mm, suggesting its ability to interfere with fungal metabolism. The Ni(II) and Co(II) complexes demonstrated moderate activity, while the Mn(II) complex exhibited lower efficacy, indicating reduced interaction with fungal cells. The free ligand (LH) showed limited activity, emphasizing the enhanced antifungal effects upon metal coordination. Notably, these metal complexes surpassed the standard antifungal agent Amphotericin B, which exhibited inhibition zones of 27 mm and 26 mm, highlighting their potential as superior antifungal agents (Table 3).

Conclusion

We synthesized (LH) and its metal complexes. Structural and spectroscopic description using TGA, ^{1}H and ^{13}C NMR, IR, mass spectra, UV-Vis and magnetic moments analysis confirmed ligand formation and metal coordination. This study evaluates the antibacterial and antifungal activity of the Schiff base ligand (LH) and its metal complexes. LH and its metal complexes exhibited noticeable antibacterial activity. Co(II), Ni(II), and Cu(II) complexes showed enhanced potency due to strong metal-ligand interactions. Cu(II) had the broadest spectrum, while Fe(II) and Zn(II) showed moderate effects. The antifungal efficacy of LH metal complexes exceeded Amphotericin B, with Cu(II), Zn(II) and Fe(II) exhibiting the strongest inhibition, while Ni(II) and Co(II) displayed moderate activity, and Mn(II) minimal activity.

Acknowledgments

The authors express their heartfelt gratitude to the Director of the Indian Institute of Chemical Technology, Hyderabad, the Principal of Chaitanya Deemed to be University, Hanumakonda, and the Director of the Centre for Cellular and Molecular

Biology, Hyderabad, for their invaluable assistance in providing spectral data and facilitating biological activity studies in various forms.

Supplementary Information

Supplementary information is available in the website https://nopr.niscpr.res.in/handle/123456789/5877.

References

1 Zoubi W A & Ko Y G, *App Organomet Chem*, 31 (2017) 3574.
2 Zhang J, Xu L & Wong W.Y, *Coord Chem Rev*, 355 (2018) 180.
3 Jia Y & Li J, *Chem Rev*, 115 (2014) 1597.
4 Das M, Baig F & Sarkar M, *RSC Adv*, 6 (2016) 57780.
5 Prasad K S, Castro J O, Frau J, Flores-Holgu N, Shruthi G, Shivamallu C & Glossman-Mitnik D, *J Mol Struc*, 1191 (2019) 17.
6 Wood J M, *Nat Wissen Schaften*, 62 (1975) 357.
7 Jarrahpour A, Khalili D, De Clercq E, Salmi C & Brunel J, *Molecules*, 12 (2007) 1720.
8 Wang Q, Wang Y & Yang Z Y, *Chem Pharm Bull*, 56 (2008) 1018.
9 Johari R, Kumar G, Kumar D & Singh S, *J Ind Coun Chem*, 26 (2009) 23.
10 Mittal P & Uma V, *Der Chem Sinic*, 1 (2010) 124.
11 Kesharwani R & Singh P, *Asian J Chem*, 12 (2000) 23.
12 Kumar H & Chaudhary R, *Der Chem Sinic*, 1 (2010) 55.
13 Habib S.I, Baseer M.A & Kulkarni P.A, *Der Chem Sinic*, 2 (2011) 27.
14 Bajpai P, Agrawal P K & Vishwanathan L, *J Sci Ind Res*, 41 (2011) 185.
15 Sullivan J F, J Nutr, 109 (1979) 1432.
16 Alaaddin C, Ibrahim Y, Habibe O & Misir A, *Trans Met Chem*, 27 (2002) 171.
17 Patel A.D & Joshi J D, *Syn React Inorg Met Org Nano Met Chem*, 25 (1995) 991.
18 Kriza A, Reiss A, Forea S & Carproin T, *J Ind Chem Soc*, 77 (2000) 207.
19 M Fujita, Y.J Kwon, S Washizu, Ogura K, J Amer Chem Soc, 116 (1994) 1151.
20 Konstantinovic S.S, Radovanovic B.C, Cakic Z & Vasic V, *J Serb Chem Soc*, 68 (2003) 641.
21 Farooque M A, Mosaddik M A, Islam M S, Alam M S & Bodruddoza M A K, *Online J Bio Sci*, 2 (2002) 797.
22 Patel K M, Patel K N, Patel N H, Patel M N, *Synth React Inorg Met-Org Nano-Met Chem*, 31 (2001) 239.
23 Gautam R K, Singh C P, Saxena R & Rao D P, *Eur Chem Bull*, 8 (2019) 387.
24 Shanty A A, Philip J E, Sneha E J, Kurup M R P, Balachandran S & Mohanan P V, *Bioorg Chem*, 70 (2017) 67.
25 Pontiki E, Hadjipavlou-Litina D & Chaviara A T, *J Enzy Inhib Med Chem*, 23 (2008) 1011.
26 Amer S, El-Wakiel N & El-Ghamry H, *J Mol Struct*, 1049 (2013) 326.
27 El-Wakiel N, El-Keiy M & Gaber M, *Spectrochim Acta A Mol Biomol Spec*, 147 (2015) 117.
28 Turan N, Türkyılmaz M, Güven K & Ercan A, *J Mol Struc*, 1225 (2021) 129101.
29 Yazdanbakhsh M & Takjoo R, *Struc Chem*, 19 (2008) 895.
30 NUNez-Montenegro A, Carballo R & Vázquez-López E M, *Polyhedron*, 27 (2008) 2867.
31 Zangrando E, Islam T T, Islam M A A A, Sheikh M C, Tarafder M T H & Miyatake R, *Inorg Chim Acta*, 427 (2015) 278.
32 Mohammed R M, Mahdi H A, *Hist Med*, 9 (2023) 1065.
33 Mumit M A, Islam M A A A, Sheikh M C, Miyatake R, Mondal M O A & Alam M A, *J Mol Struc*, 1178 (2019) 583.
34 Hamid S J & Salih T, *Drug Des Dev Ther*, 16 (2022) 2275.
35 Singh A, Gogoi H P, Barman P & Guha A K, *Appl Organomet Chem*, 36 (2022) 66.
36 Khan S, Alhumaydhi F A, Ibrahim M, Al-Qahtani A S, Alshamrani M & Alruwaili A S, *Anticancer Agents Med Chem*, 22 (2022) 3086.
37 Shukla M, Kulshrashtha H & Seth D S, *Int J Mat Sci*, 12 (2017) 71.
38 Iacopetta D, Catalano A, Cirillo F, Lappano R & Sinicropi M S, *Antibiotics*, 11 (2022) 191.
39 Bitu M N, Hossain M S, Zahid A A, Zakaria C M, Kudrat-E-Zahan M, *Am J Heterocycl Chem*, 5 (2019) 11.
40 Hossain M S, Roy P K, Zakaria C M, Kudrat-E-Zahan M, *Int J Chem Stud*, 6 (2018) 19.
41 Nagata T, Yorozu K, Yamada T & Mukaiyama, *Angew Chem Int Ed Eng*, 34 (1995) 2145.
42 West D X, Ives J S, Krejci J, Salberg M M & Zumbahlen, *Polyhedron*, 14 (1995) 2189.
43 Frei A, Zuegg T, Elliott J, Baker J, Eckhardt K, Prinz L L, Cooper H R & Keene M F, *Chem Sci*, 11 (2020) 320.
44 Zafar W, Ashfaq M, Asghar F, Tabassum A B, Afzal M, Sher M A, Ali S, Afzaal M, *Eur J Med Chem*, 210 (2021) 112981.
45 Joshi R, Kumar A, Sharma S, Sharma P K, Patel M, Batra B K & Jain R, *J Mol Struc*, 1221 (2020) 128823.
46 Grytsai O, Zayats M, Kravchenko Y, Chumak V, Senchik I, Lukianchuk A S, Kolesnyk I M, *Bioorg Chem*, 105 (2020) 104413.
47 El-Sebaey S A, *Chem Sel*, 5(2020) 11812.